AD NUMBER

AD417361

LIMITATION CHANGES

TO:

Approved for public release; distribution is unlimited.

FROM:

**Distribution authorized to U.S. Gov't. agencies and their contractors;
Administrative/Operational Use; 20 AUG 1963.
Other requests shall be referred to Office of Naval Research, Arlington, VA 22203.**

AUTHORITY

ONR ltr dtd 25 Apr 1966

DISCLAIMER NOTICE

THIS DOCUMENT IS THE BEST QUALITY AVAILABLE.

COPY FURNISHED CONTAINED A SIGNIFICANT NUMBER OF PAGES WHICH DO NOT REPRODUCE LEGIBLY.

Contract Nonr 3437(00)

Semiannual Technical Summary Report

Period Ending 20 August 1963

"STABLE DENSE COLD PLASMA"

Advanced Research Projects Agency
Order No. 194, Amendment No. 2
Project Code No. 3980
Issued February 20, 1963 to
Unified Science Associates, Inc.

Project Scientist: Dr. S. Naiditch
Telephone No. MUrray 1-3486

UNIFIED SCIENCE ASSOCIATES, INC.

826 south arroyo parkway
pasadena, california
murray 1-3486

417361

Dr. S. Maiditch presented a paper on the conductivity of sodium-ammonia solutions at the Weyl Colloquium, held at Universite Catholique, Lille, France. The principal results to date are given in the appended paper, which will be published in the Proceedings of the Colloquium.

We have now turned our attention to obtaining data for clarification of the nature of the sodium-ammonia solutions. In particular, we are modifying our system so that we can vary the pressure on the solutions. The significance of the pressure measurements may be seen from equations on page 45 of the attached paper. Here it will be noted that we have been measuring conductivities as functions of temperature along the vapor pressure curve. If we can measure the effects of pressure on the conductivity as well as the vapor pressure itself, we can then deduce the temperature coefficient of conductivity at constant pressure and composition. Preliminary experiments, initiated to enable us to check the validity of carrying out this program, have been encouraging.

PLANS FOR NEXT QUARTER

The modifications for the pressure studies should be completed and experimental measurements initiated in the next quarter.

A system for measuring density coefficients should also be made operational. The density temperature coefficients are also needed for interpretation of the data since specific conductivities are based on number densities rather than on compositions.

Distribution List for Semiannual and Final Technical Summary Reports

Agency	No. of copies
Director Advanced Research Projects Agency The Pentagon Washington 25, D.C.	6
Chief of Naval Research Department of the Navy Washington 25, D.C. Attn.: Code 429	2
Commanding Officer Office of Naval Research Branch Office 1030 East Green Street Pasadena 1, California	1
Chief, Bureau of Naval Weapons Department of the Navy Washington 25, D.C. Attn: RRRE-6	1
RAPP-33	1
RAAE-511	1
DLI-3	1
Space Sciences Laboratory Litton Systems, Inc. Beverly Hills, Calif.	1
AVCO-Everett Research Laboratory Everett, Massachusetts	1
Plasma Propulsion Laboratory Republic Aviation Corp. Farmingdale, New York	1
Stevens Institute of Technology Hoboken, New Jersey Attn: Winston H. Bostick	1
Astro Electronics Division RCA Laboratories Radio Corporation of America Princeton, New Jersey	1

Agency	No. of copies
Allison Division General Motors Corporation Indianapolis, Indiana	1
Research Laboratories United Aircraft Corporation East Hartford 8, Connecticut	1
Cambridge Research Laboratory L G. Hanscom Field Bedford, Massachusetts	1
Electro-Optical Systems, Inc. 125 North Vinedo Avenue Pasadena, California	1
Space Sciences Laboratory Missile and Space Vehicle Dept. General Electric Company Philadelphia 24, Penna.	1
Geophysics Research and Development Center University of Maryland College Park, Maryland	1
Plasma Flow Section NASA, Lewis Research Center Cleveland 35, Ohio	1
Experimental Physics Dept. Aeronutronics Ford Motor Company Newport Beach, California	1
California Institute of Technology 1201 East California Street Pasadena, California Attn: Robert G. Jahn	1
Plasmadyne Corporation Santa Ana, California	1
The Pennsylvania State University University Park, Pennsylvania Attn: Dr H. Li	1
Gas Dynamic Laboratory Northwestern University Evanston, Illinois Attn: Dr. All Cambel	1

Agency	No. of copies
Physics and Advanced Systems Dept. Reaction Motors Division Thiokol Chemical Corp. Denville, New Jersey	1
Atlantic Research Corporation Alexandria, Virginia	1
Armed Services Technical Information Agency Arlington Hall Station Arlington 12, Virginia	10
Office of Technical Services Department of Commerce Washington 25, D.C.	1
Professor E. Charles Evers Associate Professor of Chemistry University of Pennsylvania Philadelphia, Penna.	1
Hughes Research Laboratories 3011 Malibu Canyon Road Malibu, California Attention: Dr. R. C. Knechtli	1
Rocket Power-Talco 3016 East Foothill Boulevard Pasadena, California Attention: Mr. M. Farber	1
Cambridge Research Laboratories Bedford, Massachusetts Attention: Code CKZAP Dr. Norman Rosenberg	1
ASRMPE-1 Aeronautical Systems Division Air Force Systems Command U. S. Air Force Wright-Patterson Air Force Base, Ohio Attention: K. E. Vickers, or 2nd LT Carl N. Capuco	1
Professor J. C. Thompson University of Texas Austin 12, Texas	1

COLD PLASMAS:

1. ELECTRICAL CONDUCTIVITIES OF SODIUM-AMMONIA SOLUTIONS

by

S. Naiditch
Unified Science Associates, Inc.
Pasadena, California

Paper presented at

Colloque Weyl
Universite' Catholique
Lille, France
24-28 June 1963

This program is being supported by the
Advanced Research Projects Agency
and the
Office of Naval Research
under
Contract No. NONR-3437(00)

Cold Plasmas.

1. ELECTRICAL CONDUCTIVITIES OF SODIUM-AMMONIA SOLUTIONS*

by

S. Naiditch
Unified Science Associates, Inc.
Pasadena, California

ABSTRACT

Electrical conductivities of sodium-ammonia solutions have been measured from -80 to +185°C, i.e., most of the liquid range and some of the gaseous range. The objective of these studies is the exploration of the possibility of using such gaseous solutions as plasma sources. The attractive features of these gases found in this study include plasma lifetimes in excess of 3,000 seconds (the plasmas being at equilibrium), temperatures as low as 134°C and electrical conductivities of at least 100 mhos/cm.

Visual appearances of the dense gases are the same as those of the liquids. Gases with low concentrations of sodium are blue and ones with high concentrations are yellow-red metallic copper-gold.

Electrical conductivities of the liquids increase with increasing temperature until conductivity maxima are reached at 80 to 100°C. In dilute solutions, the temperatures of these maxima are close to the solution critical temperatures; because of this, conductivities of supercritical gases have been measured that are higher than the conductivities of the liquids of the same mole fractions at room temperature.

* This program is being supported by the Advanced Research Projects Agency and the Office of Naval Research under Contract No. NONR-3437(00).

1. INTRODUCTION

The objective of this program is the preparation of compressible gaseous plasmas under equilibrium with high electrical conductivities. Dense gases of metals satisfy these requirements. Birch obtained conductivities in dense mercury gases as high as 1100 mhos/cm at 1400°C and 2700 kg/cm^2 (32 BIR).* Use of such dense gases for plasma studies is not attractive because of the difficulties of experimentation under these extreme conditions. Therefore, the use of dense gaseous solutions, which exist at lower temperatures than the one-component systems, is being investigated, ammonia being chosen as the gaseous solvent and metallic sodium as the solute.

* References are listed at the end of this paper.

The feasibility of the program was based on the following:

(1) Electrolytic properties of dense gaseous electrolytic solutions are similar to those of liquid solutions;

(2) Concentrated liquid sodium-ammonia solutions have metallic characteristics; and

(3) Hennay and Hogarth (80 HAN) showed that gaseous ammonia dissolves metallic sodium and that these gaseous solutions have lifetimes of at least a few seconds, the limitation arising because of the self-reaction between solvent and metal,

$$Na + NH_3 = NaNH_2 + 1/2H_2.$$

The lifetimes of the sodium-ammonia solutions in the gaseous state are of interest since, unlike most laboratory gaseous plasmas, these solutions are under equilibrium; and therefore, the only limitation on the plasma lifetime is the chemical self-reaction.

We have studied the lifetimes of gaseous solutions by sealing purified solutions in glass tubing and heating to 135-185°C. In the initial phases of the program, the removal of causes of the self-reaction between solvent and metal was stressed.

Once useful lifetimes were obtained, emphasis was switched to the measurement of the electrical conductivities in both the liquid and gaseous states since electrical conductivities are one of the most important plasma parameters. The current-potential techniques used in all the reported investigations of electrical conductivities of metal-amine solutions require the immersion of electrodes into the solutions. Contact of such electrodes with the solutions results in catalysis of the self-reaction between solvent and solute, the reaction becoming more vigorous as the temperature is increased. Kraus (21 KRA) tried substituting metals such as gold for platinum. Obtaining no appreciable improvement, he then reduced the surface area of the electrodes to a minimum and stirred the solutions in order to make the solution more uniform and to remove bubbles produced by the self-reaction. Since immersion electrodes catalyze the self-reaction, the effect becoming worse with increasing temperatures, use of immersion electrodes in the literature below has restricted conductivity measurements to low temperatures.

The most extensive sets of conductivity-concentration data in the literature are those for $Na-NH_3$ solutions, there also being data for $Li-NH_3$, $K-NH_3$, $Na-K-NH_3$ and $Li-CH_3NH_2$ solutions. Cady (97 CAD) found that sodium-ammonia solutions are excellent conductors and that there is no polarization current. He said that "the solution seems to conduct like a metal and not like an electrolyte". Franklin and Kraus (00 FRA) confirmed the experimental findings of Cady. Kraus (21 KRA) then made a definitive series of measurements of the specific conductances

of solutions of sodium, potassium, lithium, and sodium-potassium in liquid ammonia at -33.5°C at low and moderate concentrations and Kraus and Lucasse of concentrated sodium and potassium ammonia solutions at -33.5°C (21 KRA-a) and of potassium (23 KRA). More recently, Evers, Young II, and Panson (57 EVE) measured the conductances of lithium methylamine solutions as functions of concentration at -22.8°C and Berns, Evers, and Frank, Jr. (60 BER) at -78.3°C, the latter stating that decomposition of the solutions constituted a major problem in concentrated solutions at -23° and in dilute solutions at -33.5°C.

The state of measurements of conductivity temperature coefficients is less extensive. Franklin and Kraus (00 FRA) stated that the temperature coefficient of sodium-ammonia solutions was between 0.5 and 1.5% and of positive sign much below -33°C. They reported that coefficients for lithium and potassium are positive (00 FRA-a).

Kraus (21 KRA) measured the temperature coefficients of a dilute sodium-ammonia solution from -33 to +85°C and of a concentrated solution from -33 to +50°C. He was not able to reduce the rate of self-reaction sufficiently to get reproducible measurements. His results are of particular interest because the electrical conductivity increased with increasing temperature from -33 to +85°C. Kraus noted that this behavior of sodium-ammonia solutions is in striking contrast to that of normal electrolytes in ammonia. The conductances of electrolytes in ammonia pass through maxima in the neighborhood of room temperature, the conductances decreasing with increasing temperatures above this point. Kraus stated that "It is obvious that the factors involved in the temperature coefficients of the metal ammonia solutions are very different from those involved in solutions of ordinary electrolytes. It is difficult in the present state of our knowledge, to state to what the high value of the temperature coefficient is due" (22 KRA-a).

Kraus conjectures that the high value of the temperature coefficient at high temperatures is due to increased electron mobilities.

Lucasse (22 LUC) reported a few coefficients at low temperature. Kraus and Lucasse made an extended set of quantitative reproducible measurements of the conductivity temperature coefficient of solutions of sodium (22 KRA) and potassium (23 KRA) in liquid ammonia from -33 to -70°C. The temperature coefficients for potassium solutions decrease with increasing temperature.

Panson and Evers (60 PAN) measured the conductivities of moderately dilute lithium-methylamine solutions from -78 to +20°C. In the dilute solutions, conductivity maxima occur at -20° to -5°C, the temperatures of the maxima increasing with increasing concentrations. In the dilute solutions, the data were not reproducible above about -20°C, and in the moderately dilute solutions above about -10°C. They concluded their data provide direct evidence for the existance of mass action equilibrium in metal-amine solutions.

2. EXPERIMENTAL APPROACH

Our experimental investigations have been centered around solution lifetimes and conductivities at elevated temperatures. With respect to gaseous solution lifetimes, Hannay and Hogarth had prepared one sodium-ammonia solution which lasted for a few seconds in the gaseous state (SO HAN), the shortness of the lifetime was undoubtedly due to the catalysis of the self-reaction by impurities. In order to obtain longer lifetimes, we adopted techniques designed to ensure that the solutions would be in states of highest attainable purity, and that the measuring devices would not place foreign materials in contact with the solutions.

2.1 SAMPLE PREPARATION

Current ultra high vacuum philosophy has been adapted to our purification and sample preparation systems even though the operating pressures are often as high as 100 mm. These systems are thoroughly baked out at 385°C under high vacuum to remove volatilizable contaminants. All valves used inside the oven are bakeable, all-glass, non-lubricated, pack-less, and non-leaking with respect to the outside atmosphere.

Valve functions are satisfied by use of breakseals, by all-glass valves, and by final seal-off. Since contaminants are evolved under the intense heat required for seal-off, the use of this method has been restricted to the one instance where no other method can be used; namely when the conductivity cells containing the purified solution are separated from the vacuum system. Each seal-off region is isolated from the rest of the sample preparation system to prevent contamination of other cells by the seal-off products. In practice there is a bank of five units, each unit consisting of a set of two conductivity cells serviced by one condenser which is connected to and isolated from the ammonia purification system by a freeze valve. Thus, if excessive contamination is produced during seal-off of one cell, this will affect, at most, a second cell.

When a transfer-free closure is needed, the freeze valve is used. This valve is constructed in the form of a capillary U-tube. When closure is desired, ammonia is condensed in the U-tube with liquid nitrogen. This solid ammonia plug can be pumped to 10^{-5} mm. On several occasions when conductivity cells have been snapped off accidently, the sudden introduction of the atmosphere did not produce a detectable change on a discharge gauge on the other side of the freeze valve.

For less critical applications, a ground glass check valve operated by an external magnet is used. The magnet interacts with an iron slug sealed inside the glass check valve. One end of this valve can be pumped to 10^{-5} mm when the other end is at atmospheric pressure.

The sodium used for purification of ammonia and for sample preparation is prepared by triply distilling commercial bars of metallic sodium. Most sources contain liquid hydrocarbon contaminants. Liquid-free 99.99% sodium appears to have adequate purity after triple distillation; whereas, sodium under hydrocarbons requires more rigorous purification.

Metallic sodium has also been prepared from multiply-recrystallized sodium azide, the sodium being produced on heating the azide in vacuum.

$$NaN_3 = Na + 1\ 1/2N_2$$

The sodium so prepared is an excellent catalyst, solutions prepared with it decomposing at dry ice temperatures. This catalytic behavior disappears after multiple distillation of the sodium.

In the ammonia purification process, tank ammonia, Matheson Company, Inc., 99.99% minimum, is condensed outside of the oven over metallic sodium and allowed to reflux. Further purification is completed inside a bakeable vacuum system (figure 1). Outside the oven, standard components such as greased glass stopcocks, Vitron-A glass vacuum needle valves and liquid nitrogen traps are used. Inside the oven, glass is the only material that can come in contact with sodium or ammonia in the liquid or the gaseous states. After refluxing, the ammonia is distilled and the central fraction collected in a bakeable vacuum fractionating column inside the oven. After refluxing, the central fraction is

collected in a second fractionating column. The ammonium obtained after refluxing and rejection of the initial fraction is used to prepare the samples.

The freeze valves connecting the ammonia purification system to the sample preparation system are then cooled with liquid nitrogen. A breakseal between the purified ammonia and the freeze valves is now broken and ammonia is condensed in the freeze valves, thereby isolating each pair of conductivity cells from the other pairs. Encapsulated purified sodium samples, located between condensers and conductivity cells, are then opened and distilled onto the walls under high vacuum. After this, one freeze valve at a time is opened and ammonia is liquified by the condenser above the pair of cells. The condensed ammonia then washes the sodium off the walls into the conductivity cells. The lower part of the partially filled cell is immersed in liquid nitrogen, the freeze valve refrozen, the section pumped to 10^{-5} mm, the cell sealed off, the seal-off annealed, and the cell stored in dry ice.

2.2 CONTAINMENT

Studies in liquid ammonia solutions from -78 to +50°C have often been carried out in Faraday or ammonia tubes which are V-shaped tubes with a stopcock at the V. Because stopcocks require lubricants, i.e., foreign materials, we ruled out use of these tubes as high temperature cells. Instead, we adopted the technique often used to contain supercritical fluids. Generally, heavy walled glass tubes, half filled with liquid and sealed off, have been used to contain hot gases under temperatures and pressures more extreme than those required for the containment of sodium-ammonia solutions. For example, Kistiakowsky used quartz tubes to contain pressures of about 300 atmospheres at 300°C (28 KIS). In contrast to this usually adequate behavior of glass, however, the performance of glass for the containment of hot dense sodium-ammonia fluids has been unsatisfactory.

Although the usual cause of failure of glass tubes containing dense gases is mechanical failure arising from inadequate annealing of the glass, we feel our problems have arisen from other causes. For example, not only have we been very careful in annealing the pyrex; but we have also tried using quartz, in which the strain problem is less significant than with pyrex. We found that neither the careful annealing of pyrex nor the use of quartz eliminated the difficulty.

Another source of strain, inhomogeneity of glass in the seal-off region, was the cause of many failures. Frequently, there was sufficient sodium deposited on the walls in the seal-off region to react with the glass during seal-off and to weaken the glass cell seriously. This problem has been eliminated by [illegible] of the cells under vacuum. One consequence of this treatment is that the solutions flow down the walls freely without leaving appreciable amounts of deposits.

The mechanical strength of the glass is influenced by microcracks on the surface, these cracks acting as stress multipliers (20 GRI) (60 KOH) (61 BEZ). The strength of glass may be increased by as much as a factor of ten by using a hydrofluoric acid wash which removes the surface layer. In addition to removing surface microcracks, this treatment has the additional benefit of removing sorbed surface layers of alkali hydrates, which form on exposure of glass to the atmosphere (this layer being the principal source of prolonged outgasing during bake-out under pumping). No improvement resulted from use of the hydrofluoric acid wash.

A fourth source of strain is the presence of internal pressures of hundreds of atmospheres inside the cells at elevated temperatures, which set up stresses in the glass. These stresses weaken the glass, since glass under tension is mechanically weak. Since glass under compression is strong, external pressurization has been introduced; however, this has not provided a complete solution to the rupture problem.

Besides mechanical effects, strain reduces resistance to chemical attack. Thus, Holley, Neff, Weiler and Winslow (62 HOL) report that pyrex exposed to cesium vapor at 400°C for 240 hours is badly attacked at the strain points. In addition, the regions where glass has been blown appear to be more suseptible to attack. Vycor, after exposure to cesium vapor for one hundred hours at 400°C, is fractured due to attack at joints; and aluminum borosilicate glass, after fifty hours at this temperature, is found to be slightly oxidized at joints. Thus, it is possible that the most deleterious effect of strain is not the reduction in the mechanical strength of the glass, but the reduction in resistance to chemical attack.

The following glasses are presently under evaluation for usability

The mechanical strength of the glass is influenced by microcracks on the surface, these cracks acting as stress multipliers (20 GRI) (60 KOH) (61 BEZ). The strength of glass may be increased by as much as a factor of ten by using a hydrofluoric acid wash which removes the surface layer. In addition to removing surface microcracks, this treatment has the additional benefit of removing sorbed surface layers of alkali hydrates, which form on exposure of glass to the atmosphere (this layer being the principal source of prolonged outgasing during bake-out under pumping). No improvement resulted from use of the hydrofluoric acid wash.

A fourth source of strain is the presence of internal pressures of hundreds of atmospheres inside the cells at elevated temperatures, which set up stresses in the glass. These stresses weaken the glass, since glass under tension is mechanically weak. Since glass under compression is strong, external pressurization has been introduced; however, this has not provided a complete solution to the rupture problem.

Besides mechanical effects, strain reduces resistance to chemical attack. Thus, Holley, Neff, Weiler and Winslow (62 HOL) report that pyrex exposed to cesium vapor at 400°C for 240 hours is badly attacked at the strain points. In addition, the regions where glass has been blown appear to be more suseptible to attack. Vycor, after exposure to cesium vapor for one hundred hours at 400°C, is fractured due to attack at joints; and aluminum borosilicate glass, after fifty hours at this temperature, is found to be slightly oxidized at joints. Thus, it is possible that the most deleterious effect of strain is not the reduction in the mechanical strength of the glass, but the reduction in resistance to chemical attack.

The following glasses are presently under evaluation for usability

as cell materials at elevated temperatures.

Pyrex	Corning Code No. 7740
Quartz	Engelhard Industries; General Electric
Uranium Glass	Corning Code No. 3320
Aluminosilicate	Corning Code No. 1720
Kovar Sealing Glass	Corning Code No. 7052

So far, the behavior of quartz has been similar to pyrex. One glass, Corning No. 7052, has exhibited relatively poor strength. Another, Corning No. 1723, is difficult to work with and to seal after filling with solution. A suitable glass must exhibit resistance to chemical attack (i.e., to rupture) and must not affect solution lifetimes (i.e., be non-catalytic and produce no soluble contaminants).

It is felt at this time that chemical attack of the hot solutions may be the prime source of the containment difficulty. It has been found that with concentrated solutions rupture occurs at lower temperatures than with the dilute ones. Use of external pressurization mitigates, but does not entirely solve the rupture problem. The complete external pressurization assembly is shown in figure 3.

2.3 ELECTRICAL CONDUCTIVITY MEASURING SYSTEM

The conductivity measuring system was designed so that glass would be the only foreign material in contact with the solutions. Two types of inductive electrical conductivity measurement techniques were evaluated, one with solutions in straight tubes of glass and the second in toroids. From the viewpoint of accuracy, the toroidal technique proved to be superior and was adopted.

The sodium-ammonia solutions are contained in conductivity cells having a toroidal end (figure 2). A coil is wound about a ferrite torus, which is linked through the conductivity cell torus, which is linked in turn through an output ferrite torus with a coil wound about it. An input signal induces a current in the conductivity cell torus which induces a current in the output coil. The assembly inside the bomb is shown in figure 4. An internal heater is located parallel to, but below the conductivity cell, and an external heater is placed on the outside of the bomb.

The transfer function across the system is dependent, not only on the geometry and conductivity of the sample, but also on the frequency of the measuring signal. For each range of cell resistances, there is an optimum frequency range for maximum sensitivity and accuracy. For these reasons, the approximate conductivity of the solution torus is determined and the correct frequency used for that sample, as in table I.

The conductivity measuring system is calibrated with toroids fabricated accurately either with liquid mercury or solid resistive materials or with toroids which include fixed resistors or resistance boxes in their circuits. When calibrating the system, these toroids are placed between the ferrite toroids in the position normally occupied by the conductivity cells. The transfer functions for the liquid and solid toroids are in quantitative agreement with each other.

3. VALIDATION AND TREATMENT OF EXPERIMENTAL DATA

Initial effort has been on the removal of causes that prevent the data from being reproducible. In addition, it has been necessary to detect when spurious effects are occurring, and to either eliminate these effects or to discard the data when such effects are present. The limits of accuracy attainable in the absence of spurious effects have also been established. The principal troublesome effects have been decomposition of solutions, instrumental malfunctioning, and erratic behavior near the critical point.

3.1 REPRODUCIBILITY OF THE DATA

In order to establish the validity of the experimental data, it is essential to establish whether or not the conductivity data are reproducible. In more recent high temperature runs, samples have been cooled occasionally during the heating cycle to determine whether or not measurable decomposition has taken place.

The heating system has been modified so that small temperature drops can be produced rapidly when desired. In addition to dropping the temperature at intervals to detect when measurable decomposition of the solution has started, the temperature is also dropped whenever there is a sudden change of conductivity, to see whether decomposition is associated with the change. In figure 5, recent reproducibility data are shown for two samples which were each heated three separate times. There is no detectable change in conductivities produced by these heatings, confirming that it is possible to make high temperature conductivity measurements under reproducible conditions to at least +130°C. Behavior of data in runs such as 10-30-3 (figure 8) indicate that reproducible data have been achieved at temperatures of 165°C.

3.2 ERRATIC BEHAVIOR OF THE SOLUTIONS

In earlier experiments, the conductivity cells were fabricated from heavy walled pyrex capillary and tested in the atmosphere behind glass barricades. Vigorous turbulence was often observed just below the critical points; at the same time, the conductivity data became erratic, varying by as much as a factor of ten over a period of a few minutes. Effects of this turbulence are often observed in the more recent experiments in which the conductivity cells are externally pressurized in a bomb. Results of this turbulence are indicated in Figure 9. Bubbles appeared in the capillary at the same time that sudden increases in solution resistance occurred. This problem has been eliminated by use of larger diameter tubing when the external pressurization bomb is used.

3.3 INSTRUMENTAL MALFUNCTIONING

Because of the corrosiveness of the solutions, there have been many difficulties with instrumentation. When cells at temperatures of 150 to 200°C rupture, the sodium-ammonia solutions are released and react with the instrumentation in the interior of the bomb. Bad junctions or even electrical open circuits are often produced. Hence, the system is now cleaned and checked-out after each run. Whenever the check-outs are unsatisfactory, the wiring is corrected.

Since failures also occur occasionally during runs on the systems that check-out satisfactorily, a device was installed for calibrating the conductivity measuring fixture at high temperatures and pressures while the run is in progress. This external calibrator consists of a wire torus which is electrically parallel to the conductivity cell torus and which is connected, through a switch, to an external resistor. When the switch is open, the torus circuit is open; when the switch is closed, the torus is closed through the external resistor.

3.4 CONDUCTIVITY MEASURING TECHNIQUE

The purpose of the reduction of the data is to determine the specific conductivity of the solution, σ, as a function of the temperature, t, and the mole fraction of sodium, x_2. The steps in the process for calculating σ are:

(i) calibration of the conductivity measuring system
(ii) calibration of conductivity cell
(iii) measurement of the solution resistances and temperatures.

The conductivity measuring system is calibrated with toroids made from solid materials (secondary standards) and from liquid mercury. Use of liquid mercury toroids provides additional confidence in the general conductivity measuring technique since mercury, like the sodium-ammonia solutions, is a liquid conductor. In addition, the mercury toroids are carefully constructed and calibrated for use as primary standards. The calibrations based on the solid resistors agree quantitatively with those for the mercury toroids.

The purpose of calibrating the conductivity cell is to establish the ratio, C, of the resistance of a solution in the cell torus to its resistivity. The following techniques have been used to calibrate the conductivity cells:

(i) Geometrical

The cell constant is equal to the total length of the torus divided by the cross-sectional area of the glass tubing. Because the cells are glass-blown, there are many irregularities in the torus, so that this method of measuring the cell constant is less accurate.

(ii) Direct Current Plunger

A plunger is inserted into the cell, blocking electrical continuity in the torus. The blocked torus is filled with mercury and the direct current conductivity measured. The cell constant is the ratio of the resistance, corrected for the presence of the plunger, to the resistivity of mercury.

(iii) Inductive Method Using Liquid Mercury

The cell is filled with mercury and the resistance measured inductively. The cell constant is the ratio of this resistance to the resistivity of mercury. The highest accuracy is attainable with this method. Since the conductivities of the solution and mercury in the same cell are both measured with the same technique, one obtains the ratio of conductivities of solution to mercury directly. The transfer function constant cancels out rather than contributing an error in the final determination of the solution conductivities.

A number of operational procedures have been used to calibrate the conductivity fixture and to measure the solution resistances. In the calibration procedure, known toroidal resistors are placed through the two ferrite cores, and the transfer functions measured. Then a conductivity cell is placed in the fixture, and the transfer functions measured again. The ratio of transfer functions of cell to standard are equal to the ratios of their resistances. The following procedures have been used:

(1) Initially, a graphical technique was used. The

output voltage, V^o, is plotted against the toroidal resistance, R, at constant input voltage, V^i, and frequency, ν.

(2) Next, the fact that $\frac{RV^o}{\sqrt{V^i}}$ is constant was used (the V^o technique).

(3) More recently, the external calibrator has been used. This places a torus with a known resistance in parallel (electrically) with that of the solution torus.

(4) In addition, a figure-eight torus has been used such that the current it transfers is in opposition to that transferred by the conductivity cell. A minimum or null output results when the two resistances become equal.

Use of the graphical technique was dropped in spite of its obvious advantage that over a small resistance range it can give greater accuracy than the other techniques. Its principal disadvantages are that the voltage resistance function becomes two valued and the sensitivity is reduced when the resistance becomes either relatively large or small. Thus, it could not be used to calibrate conductivity cells filled with liquid mercury or with concentrated sodium-ammonia solutions. For these reasons, we examined the behavior of the conductivity measuring system experimentally, and developed the V_o method.

Within small ranges of resistance at an optimum frequency which is a function of the resistance, the output voltage is directly proportional to the reciprocal of the resistance of the torus. This method proves to be convenient in practice, because a minimum of data processing is involved. The output voltages are plotted directly as functions of temperature, then the ordinate scale is shifted once. On the new scale we now have specific conductivity as a function of temperature.

The most important difficulty associated with the V_o technique is that the optimum frequency shifts during the run since the resistance of the solution changes. For most cases, this change in resistance at constant frequency may lead to an error of less than 1 or 2% in specific conductivity. It is possible to remove this source of error by determining the optimum frequency at each temperature; however, this is not feasible because of the excessive time it takes to determine the optimum frequency. This is especially a problem at elevated temperatures when the time to carry out the experiment is seriously restricted.

Another difficulty with the V_o technique is that when peculiar effects arise, one cannot always distinguish between real and spurious effects. In fact, the external calibrator technique was

developed because on one run the output voltage suddenly dropped indicating either that the glass cell had ruptured or that the solution had decomposed completely. When the bomb was cooled and opened, it was found that the cell was intact and the solution was dark blue. What had happened was that there had been an instrumental failure within the bomb. The external calibrator was developed and installed so that we could calibrate the conductivity measuring system during operation. This device has proved invaluable for distinguishing between instrumental failures and other effects.

Another real advantage of the external calibrator is that it is not affected by small shifts in calibration in the conductivity measuring system as the temperature is changed. The external calibrator has a disadvantage in that the optimum frequency for the conductivity cell is different than that for cell plus calibrator. However, in evaluating this experimentally, it has been found that this situation generally does not produce noticeable effects.

A null technique has also been used, in which a figure-eight external calibrator torus is placed antiparallel (electrically) to the solution torus. Hence the power transferred from one ferrite torus to the other by the null torus opposes that transferred by the solution torus. When this technique has been used, the output voltage is minimized when the resistance of the external null torus is approximately equal to that of the standard calibration torus; the output voltage, however, is still relatively large. The difficulty with this technique has been that it requires a large amount of time to collect the requisite data. The advantage is that it is accurate even if the frequency is not optimal but close to optimal.

In practice, the following two techniques are used simultaneously. When the external calibrator technique is being used, the data automatically apply to the V_o technique, so that a single set of data can be reduced using both approaches. Generally, the agreement between the two techniques is within a few percent.

3.5 REDUCTION OF DATA

The equations used for data reduction will be summarized since they are needed for the error analysis that follows. The calibration of conductivity cells is made to determine the cell constant, C, where $C = \kappa R$.

(a) Geometrical: $$C = \sum_i \frac{\ell_i}{A_i}$$

For the glass cells the approximation has been made that $C = \ell/A$ where ℓ is total toroidal path length and A is the internal diameter of the glass from which the cell is fabricated. For the precision plastic Hg cells, ℓ and A are measured accurately; the only significant errors are due to the presence of the four corners formed from the intersections of the cylinders of the rectangular toroids.

(b) Direct Current Plunger (current-potential method) using mercury

$$R = (1 + Q)\, E/I = C/\kappa \text{ (Hg)}$$

where Q is the correction term for the presence of the plunger.

(c) Inductive Method Using Mercury

$$R = B\sqrt{\frac{V^i}{V^o}} = C/\kappa \text{ (Hg)}$$

where B is the experimentally determined constant for the conductivity measuring system.

The conductivity measuring system is calibrated as follows:

(1) The Graphical Technique

The output voltage is measured and plotted as a function of toroidal resistance at fixed frequency and input voltage.

(2) The V^o Technique

A number of toroids of Hg or of solid resistors are placed in the fixture and V^i, V^o, ν measured as functions of ν .

Then, $B = \frac{RV^o}{\nu V^i}$

We have three separate conductivity measuring fixtures, each made with the same ferrite materials, type of shielding and number of turns of coil wound on the ferrites. The values of B for the three fixtures differ by less than 2%.

The resistances of the solutions in the toroids have been measured as follows:

(1) Graphical

The output voltage, V^o, is measured at fixed frequency and input voltage. Then the solution resistance is determined from the calibration curve (except for relatively large or small R, where the function becomes two valued).

(2) The V^o Method

The resistance is determined by measuring V^i, V^o, ν and using the relation,

$$R = B \frac{\nu V^i}{V^o}$$

(3) External Calibrator

V^o and V^+ are measured, where V^+ is the output voltage when the external calibrator circuit is closed, placing this torus in parallel electrically with that of the solution torus. It is assumed (the assumption having been checked with known resistors) that

$$\frac{1}{R^+} = \frac{1}{R_{ec}} + \frac{1}{R_s}$$

where R_{ec} is the resistance of the external calibrator torus and R_s that of the solution torus.

The variables B, ν, V^i are kept constant during the process of connecting and disconnecting the external calibrator. Hence,

$$R_s = R_{ec} \left[\frac{V^+ - V^o}{V^o} \right]$$

3.6 PROPOGATION OF ERROR ANALYSIS

We shall examine two extreme cases, namely ones in which the techniques used in the calibration of the conductivity cells, the calibration of the conductivity measuring system and measurement of the solution resistance are as dependent on each other as possible and then as independent as possible. These two extremes will be examined with respect to the specific conductivity of solutions at 20°C, the temperature at which the fixture is calibrated as well as the base temperature of the experiments. Because of the latter, it will be assumed that optimal frequencies are used.

For the dependent case assume that the cell is calibrated inductively with mercury then

$$C = \sigma_{(Hg)} \left(\sqrt{\frac{V^i}{V^o}}\right)_{Hg}$$

When the solution is placed in the same cell, the resistance of the solution is given by

$$R_s = \left(\sqrt{\frac{V^i}{V^o}}\right)_s$$

and the specific conductance of the solution by

$$\sigma_s = C/R_s.$$

Then,

$$\sigma_s = \sigma_{(Hg)} \frac{\left(\sqrt{\frac{V^i}{V^o}}\right)_{Hg}}{\left(\sqrt{\frac{V^i}{V^o}}\right)_s}$$

The error, $(\delta\sigma/\sigma)_{Hg}$, is negligible compared to the errors in voltages and frequencies. The measuring instruments need only provide correct ratios, e.g., $\nu\,(Hg)/\nu_s$, rather than absolute values. Hence, the following treatment, that of using the errors of the individual terms rather than of the ratios, is conservative.

$$\left(\frac{\delta\sigma_s}{\sigma_s}\right)^2 \leq 2\left(\frac{\delta\nu}{\nu}\right)^2 + 4\left(\frac{\delta V}{V}\right)^2.$$

The more independent case will now be examined. The cell is calibrated non-inductively, the conductivity system is calibrated by the V^o method and the measurements made using the V^o method. Then

$$\sigma_s = C/R_s$$

$$R_s = B\nu\frac{V^i}{V^o} \text{ and } R_c = B\left(\nu\frac{V^i}{V^o}\right)_c$$

so that

$$\left(\frac{\delta\sigma_s}{\sigma_s}\right)^2 \leq \left(\frac{\delta C}{C}\right)^2 + \left(\frac{\delta R_c}{R_c}\right)^2 + 2\left(\frac{\delta\nu}{\nu}\right)^2 + 4\left(\frac{\delta V}{V}\right)^2$$

The error in this approach is greater than in the previous one because of the presence of two additional terms, one involving the error of the cell calibration and the other the error of the values of the resistances of toroids used for calibration. For this reason, the inductive method of calibration of the conductivity cells has been used ever since we were able to extend the range of the inductive measuring technique to low resistances.

In addition to the accuracy of the determination of specific conductivity, we are also interested in that of the function, E_σ, which is defined by

$$\frac{E_\sigma}{R_g} = - \frac{d \ln \sigma}{d \theta}$$

where R_g is the gas constant
and θ is the reciprocal of the absolute temperature, $^oK^{-1}$.

Let us assume that the cell constant, C, is constant over the range of temperatures and pressures used; also, that the frequency, ν, and the input voltage, V^i, are kept constant during the run. The conductivity measuring system constant, B, will vary with the temperature for two reasons, the electrical characteristics of the system itself are slightly temperature dependent and the frequency becomes non-optimal as the solution resistance varies with temperature. If the V^o method is used,

$$\sigma = \frac{C}{\nu V^i} \frac{V^o}{B}$$

and

$$\frac{E_\sigma}{R_g} = \frac{d \ln \frac{B}{V^o}}{d \theta} .$$

If the external calibrator method is used, the error in B is due only to the frequency effect, since both B^o and B^+ are at the same temperature.

$$\sigma = \frac{C}{R_{ec}} \frac{V^o}{\frac{B^o}{B^+} V^+ - V^o}$$

and

$$\frac{E_\sigma}{R_g} = \frac{d \ln \frac{\frac{B^o}{B^+} V^+ - V^o}{V^o}}{d \Theta}$$

It is immediately apparent from a comparison of the equations for E_σ with those for σ, that the most important sources of error are different for E_σ than for the specific conductivity. The relative errors in E_σ are respectively

$$\left(\frac{\delta E_\sigma}{E_\sigma} \right)^2 = \left(\frac{\delta \Theta}{\Theta} \right)^2 + \left(\delta \ln \frac{d \ln \frac{B}{V^o}}{d \ln \Theta} \right)^2$$

and

$$\left(\frac{\delta E_\sigma}{E_\sigma} \right)^2 = \left(\frac{\delta \Theta}{\Theta} \right)^2 + \left(\delta \ln \frac{d \ln \left(\frac{B^o}{B^+} \frac{V^+}{V^o} - 1 \right)}{d \ln \Theta} \right)^2 .$$

We have expanded the last term on the right for the V^o method and made estimates of the component errors, deducing the following value

$$\frac{\delta E_\sigma}{E_\sigma} < 4\% .$$

The error equation for E_σ for the external calibrator method contains only ratios of B's and of voltages. The B's for each set of ratios are at the same temperature. Each pair of voltages are read one after the other on the same scale of the meter. Hence the error in E_σ for the external calibrator method is less than for the V^o method.

4. EXPERIMENTAL RESULTS

Initially the program was concerned with finding out whether useful plasma lifetimes could be realized with gaseous sodium-ammonia solutions. Next, several materials studies were carried out. The first of these studies, that with silane films, was designed to see whether we could use metal containers and electrodes. The lack of positive results forced us to use glass containers, which proved to be only partially satisfactory at elevated temperatures. Because of the use of glass, it became necessary to use an inductive technique for measuring conductivities. We were then able to obtain reproducible conductivity data at temperatures at least as high as 165°C.

4.1 LIFETIMES

When the program was initiated, the only information in the literature on sodium-ammonia solutions in the gaseous state was that of Hannay and Hogarth (80 HAN), who succeeded in producing a gaseous solution for a few seconds. The first question that had to be answered in our program was whether useful lifetimes could be attained in the gaseous state. The approach we used was predicated on the assumption that impurities were the cause of the short lifetime obtained by Hannay and Hogarth. In our program, longer and longer gaseous lifetimes were attained as experimental techniques improved. When we measured a lifetime of 52 minutes in the gaseous state at 145°C before self-reaction became observable, we then went on to the next phase of this program. We feel that we have not reached the limits of lifetimes in the gaseous state and that considerably longer lifetimes may well be attainable if needed.

4.2 MATERIALS

Three materials studies have been made, the first on coatings; the second, on glass; and the third on regeneration of solutions.

The purpose of the first materials study has been to see if we can find a non-catalytic coating for metals - so that we can place metals in contact with the solutions without catalysis. When practical coatings are developed, metal containers can be used with the mechanical advantages that metals provide. In addition, if the coatings are non-resistive, then current-potential measurements can be used instead of inductive techniques.

The behavior of silane coatings, prepared from Beckman Desicote 18772, was studied since similar coatings have been used successfully at other laboratories to reduce catalysis by metals in contact with sodium-ammonia solutions at low temperatures. Such films are prepared by depositing substituted silanes on glass and other materials by hydrolytic action (51 GIL). Adsorbed water on the surface reacts with the silane producing a film of polymerized substituted siloxane integrally attached to the surface. The polar Si-O bonds apparently exhibit an affinity for the similarly constituted glass surfaces and the organic radicals are directed outward. E. P. Arthur (51 GIL) found that a hydrolyzed silane layer does not impair the pH response of glass electrodes or appreciably increase their resistance.

Whenever silane coated materials were placed in the test cells containing sodium-ammonia solutions and the cells heated, vigorous bubbling occurred in the regions of the silane surfaces. The solutions in these regions seemed to decompose more rapidly than elswhere; therefore, tests were not continued at that time.

Because of the lack of positive results with silane films, we decided to contain our solutions in glass. We then found that pyrex is not a satisfactory material at elevated temperatures. We therefore initiated a materials study to find a way of coping with the loss in mechanical strength of glass at elevated temperatures, which is probably due to decrease in resistance to chemical attack. A variety of glasses and glass treatments have been under continual evaluation. This aspect of the program has been discussed in detail in section 2.2.

The purpose of the third materials study was to see if metallic aluminum can be used at elevated temperatures to regenerate metallic sodium used up by the self-reaction. The following reaction takes place in liquid ammonia because of the low solubility of the product aluminum amide:

$$Al + 3\ NaNH_2 = Al(NH_2)_3 + 3\ Na.$$

In addition to regeneration, the metallic aluminum and the aluminum amide catalyze the self-reaction.

When experiments were carried out at elevated temperatures with aluminum wires immersed in sodium-ammonia solutions, the regeneration took place for about an hour, but stopped before the aluminum wire was completely used up. Until that time, the rate of regeneration exceeded that of the catalyzed self-reaction. It is possible that the amide coated the surface of the aluminum, thereby stopping the reaction. Regeneration will become important when sodium-ammonia gases are used practically on a sizeable scale. In such a case, the sodium-ammonia gases could be cooled, the hydrogen produced by the self-reaction pumped off, the resulting liquid circulated through an aluminum bed, and the regenerated solution pumped back into the high temperature region.

4.3 ELECTRICAL CONDUCTIVITIES

We have measured conductivities at low temperatures in order to overlap our conductivity temperature data with the conductivity concentration data in the literature, which is at -33.5°C. Our concentrations are then established by comparison of our data at -33.5°C with the latter data. Although a gas analyzer has been installed to measure chemical compositions of the samples, too many samples have ruptured at elevated temperatures, eliminating the possibility thus far of analyses after the conductivity measurements have been completed. All concentrations reported herein have been obtained from comparison with the literature conductivity concentration data. The data in the literature are shown in the left graph in figure 6 and our low temperature data in the right graph in the same figure, as well as in Table I.

As the temperatures are raised, the conductivities pass through maxima at 80-110°C in the case of dilute solutions, whereas, the maxima flatten into plateaus at higher concentrations (figure 7 and Table II).

At temperatures above the maxima, the fractional filling of the cell at low temperature influences the observed behavior strongly. If the fractional filling is too great, the cell becomes completely filled with liquid below the critical point. Examples of this in figure 7 are runs 9-5-1A, 10-3-1A, W-1, 10-30-2A and 11-9-1. When the rising liquid fills the gas region (the intersection of this with the liquid being indicated on the curves for these runs in figure 7), the solution density becomes constant and the conductivity now rises, instead of falling, with increasing temperature.

In figure 8, the filling was approximately correct so that the transition took place near the critical region. The peculiarity

in the gas phase data below the critical point is due to the gas volume becoming partially filled with liquid as well as to long drainage times after stirring. The temperature at which gas and liquid phases became indistinguishable, 134°C, is slightly greater than that of the critical temperature of the pure solvent itself, 132.9°C. The gaseous conductivity then remained constant with increasing temperature.

The two examples of runs in which the existence of gaseous conductivities was unambiguous were runs 10-30-3 (figure 8) and 11-9-3 (figure 9) with gaseous data as follows:

GASEOUS DATA

Run No.	Mole Fraction of Sodium	Conductivity, mhos/cm	Temperature Range, °C	Approximate number density of electrons, cc^{-1}*
10-30-3	7.1×10^{-3}	7.7×10^{-1}	134 - 165	7.5×10^{19}
11-9-3	2.53×10^{-2}	1.34×10^{2}	149 - 153	2.6×10^{20}

* This estimate is based on the assumption that the sodium is fully ionized, that the gaseous solution densities are 0.3 g/cc, and that in the case of run 11-9-3 the drop in gaseous conductivity with increasing temperature was caused by the onset of the self-reaction.

Vigorous turbulence, which interferes with the collection of data in the critical regions, has been observed visually as much as 30° below the critical point when the measurements are made using capillaries. The data for six samples continued in 7 and 8 mm tubing in the bomb, in which such effects were present, are shown in figure 9. In other runs, such as in figure 8, the critical state was reached without turbulence.

in the case of solutions with intermediate concentrations, the conductivities of the liquid appear to plateau at 80 to 130°C, then to increase abruptly with increasing temperature to a new plateau (figure 10). In these runs, it was found that gaseous conductivities did not become measurable at temperatures of up to 185°C. It has not yet been established whether the effects above 130°C are real, are due to subcritical fluctuations in the liquid state or are caused by instrumental failures inside the bomb. These effects are not observed when a constant resistance torus is substituted for the cell and heated.

4.4 REVIEW OF THE CONDUCTIVITY DATA

It has been established in this program that reproducible measurements of conductivities of sodium ammonia liquid and gaseous solutions can be made at temperatures at least as high as 165°C. Insofar as the data in tables I and II are concerned,* it has become practical

* The sequence of runs shown in the tables and figures is as follows: 8-22- ; 9-5- ; W-1; X-15; 10-3- ; 10-8- ; 10-30- ; 11-9- ; 3-26- ; 4-26- ; 26; 28; 29; 33.

to properly check reproducibility only in our more recent measurements, after we had modified the apparatus for this purpose. The general behavior of the earlier runs, however, has been such that we feel that there has been measurable decomposition in at most only a few runs below 120°C.

We must consider that the reproducibility of the earlier data at elevated temperatures is generally not confirmed. The current data in runs such as those in figure 5 are reproducible and there is no evidence for believing that decomposition has set in below 165°C in such earlier runs as in figure 8.

Starting at the lowest temperatures, the first feature in the curves is the occurrence of discontinuities in the conductivity temperature curves at about -40°C (figure 6). These discontinuities occur primarily because of phase separation, but in one or two cases because of shrinkage of the solution such that a section of the torus becomes partially empty and therefore more resistive. In the case of phase separation, the conductivity drops rapidly with decreasing temperature because of the changes in compositions in the two phase region.

In the data from -80 to +20°C, the accuracies of the temperature coefficients, E_{σ} , are about 5%. The accuracies of the specific conductivities are limited primarily by the errors in cell calibration.

In the earlier measurements, there may be sizable errors in the system calibration constant, B, partially arising from the use of non-optimal frequencies. A conservative assignment of accuracies of specific conductivities might be an order of magnitude for the earlier measurements and less than 10% for the more recent ones.

At temperatures above those of the conductivity maxima (figure 7), it is possible that the relative shapes of the curves may be influenced by the initial fractional fillings of the cell. As the temperature is raised, solvent evaporates, and the liquid becomes more concentrated. The greater the initial fractional filling of the cell by the solution, the smaller the relative change by this effect since less solvent is removed from a larger volume of solution.

Consideration of other aspects of the data involves a considerable amount of speculation and is therefore deferred until the next section.

5. DISCUSSION

The three most important features of our data from which we can make deductions are:

(1) The specific conductivity, σ.

In general,

$$\sigma = \sum_i n_i q_i v_i$$

where n_i is the number density of the ith ion species,
q_i is the charge of the ith ion species,
v_i is the mobility of the ith ion species, and
the superscript "$-$" refers to electrons.

The q_i for the various species are equal to $Z_i q^-$, where Z_i is the valence of the ith ion species. The various number densities, n_i, are bounded approximately by $0 \leq n_i \leq 10 n^-$. Except for the very dilute solutions (which have not been studied by us), the mobilities of electrons are orders of magnitude greater than those of the other electrically charged species in the solutions. Since $v^- \gg v_i$ for all species and $n^- q^-$ is at most only a little smaller than $n_i q_i$ for one species, we may neglect all terms except those for the electrons, and let $\sigma = n^- q^- v^-$. From the specific conductivity, we can therefore deduce the product of electron density and mobility as a function of solution composition, temperature, and pressure.

(2) E_σ.

From the conductivity temperature data and the above specific conductivity relation, it follows that

$$-\frac{E_\sigma}{R} = \frac{d \ln \sigma}{d \Theta} = \frac{d \ln n^-}{d \Theta} + \frac{d \ln v^-}{d \Theta}$$

where Θ is the reciprocal of the absolute temperature. Unfortunately the interpretation of the data is complicated by the fact that both n^- and v^- are functions of concentration, temperature, and pressure in the sodium ammonia solutions.

Implicit equations for n^- may be derived in the form of power series,

$$\sum_{i=0}^{k} a_i (n^-)^i = 0$$

where $k \geq 2$. The coefficients, a_i, of the various powers of n^- depend on which species we assume to be present in the solution.

The a_i are functions of the equilibrium constants and a_o is in addition a function of the sodium density. Initially we are not planning to distinguish between activities and concentrations since activity coefficients are known only at low temperatures. If we let $-E_\rho/R = d \ln \rho / d \Theta$, $-\Delta H_i/R = d \ln K_i / d \Theta$, and $-E_v/R = d \ln v^- / d \Theta$, where ρ is the density of the solution and K_i the equilibrium constant for the ith equilibrium, then E_{σ} can be expressed in terms E_v, E_o, ΔH_1, ΔH_2, ... In order to complete this treatment of the data, we are now in the process of measuring the densities and vapor pressures of the sodium ammonia solutions over most of the liquid temperature range, as well as the pressure coefficients of electrical conductivity.

(5) The temperatures of the conductivity maxima.

Our preliminary interpretation of the high temperatures of the conductivity maxima is that the difference in behavior between solutions of sodium and electrolytes like NH_4I and KI in liquid ammonia is due primarily to the sodium being largely undissociated at low temperatures in the concentration range we studied and that the increase in ionization of the sodium is sufficient to compensate for the decrease in density with increasing temperature. The dissociation becomes largely complete in the neighborhood of the conductivity maxima in our more dilute solutions. Therefore, the conductivity now drops with increasing temperature since there is no longer a source of electrons to compensate for the further decrease in density.

For the intermediate concentrations, σ varies exponentially with the concentration of sodium. Thus as the solution temperature is raised, the density of sodium decreases and σ should decrease exponentially—instead it increases. It is difficult to believe that the temperature coefficient of mobility is sufficiently large to overcome this effect. Hence we are conjecturing that the electron densities are increasing with increasing temperature up to the maxima even though the sodium densities are decreasing. The source of electrons is from species variously described in the literature as e^-_2, Na, Na_2, Na^-, or polymers.

The occurrence of the maxima at 80 - 110°C is of interest, not only with respect to the cause of the increase beyond 25°, but also with respect to the effects of this increase. As pointed out previously, a very significant effect is that the temperatures of the maxima are close to those of the critical points for dilute and moderately concentrated solutions. As a result of this closeness, unlike the case for electrolytes, there is only a small drop in conductivities in going from the conductivity maxima to the gaseous state. Hence the gaseous conductivities are greater by orders of magnitude than would be the case if the conductivity maxima occurred at 25°C.

In the preceding section, we have treated the temperature coefficients as being at constant pressure, whereas the actual measurements have been made along the vapor pressure curve. In the liquid state, only the composition, such as mole fraction, or the concentration of sodium need be specified. We shall use mole fractions to specify the composition, since these are temperature independent. Assume that $\sigma = \sigma(p, T, X_2)$ for the coexistant two phase system. Then, along the vapor pressure (vp) curve,

$$\left(\frac{d \ln \sigma}{d \theta}\right)_{vp} = \left(\frac{\partial \ln \sigma}{\partial p}\right)_{T, X_2} \left(\frac{dp}{d\theta}\right)_{vp} + \left(\frac{\partial \ln \sigma}{\partial \theta}\right)_{p, X_2} + \left(\frac{\partial \ln \sigma}{\partial X_2}\right)_{p, T} \left(\frac{dX_2}{d\theta}\right)_{vp}$$

Preliminary measurements have already been carried out on the effects of pressure on conductivity at constant temperature and composition. From these results, we feel that we shall be able to determine both the vapor pressures of the solutions and $(\partial \ln \sigma / \partial p)_{T, X_2}$. Since the equation of state of ammonia gas is known, we can calculate the amounts of ammonia in the gas phase from the vapor pressures, and therefore $(dX_2/d\theta)_{vp}$. By estimating the heat of vaporization of the solution and the term $(\partial \ln \sigma / \partial X_2)_{p, T}$ from the collection of conductivity temperature concentration data, we can evaluate $\left(\frac{\partial \ln \sigma}{\partial \theta}\right)_{p, X_2}$.

We shall now return to the overall objective of this program, i.e., the plasma aspects of the gaseous sodium ammonia solutions. In the conventional nomenclature, the sodium ammonia gases are dirty plasmas, that is, they contain a foreign material, the solvent. These plasmas have gaseous conductivities of 1 to 100 mhos/cm in dilute to intermediate concentration solutions. We are now trying to prepare plasmas with considerably higher conductivities by using the more concentrated solutions. Our conviction that this can be done is based on our visual observations that we have produced gases that are metallic yellow-red copper-gold in appearance. Since the qualitative facts deduced from visual observations have already been confirmed by conductivity measurements for solutions up to intermediate concentrations, we expect that the observations on concentrated gases will also be confirmed.

The electron densities in the gaseous plasmas with conductivities of 1 to 100 mhos/cm are about 10^{19} to 10^{20} electrons per cc. The pressures, which have not yet been measured, are of the order of a hundred atmospheres. The pressures in our cold plasma are greater than those in the usual laboratory gaseous plasmas, which are at atmospheric pressure or below. In nature, there are two main sources of gaseous plasmas, the interstellar plasmas with about 10 electrons per cc and the stellar plasmas in which there is an enormous range of

densities from the tenuous red giants to the dense white dwarfs. The electron densities and gas pressures of the cold plasma would fall in the stellar class, closer to those of the red giants than the white dwarfs.

Insofar as temperature goes, there are no comparable temperatures in either the conventional laboratory gaseous plasmas or in nature. The temperatures of the interstellar plasmas may be of the order of 10^4 °C, those of the stellar interiors are very high and those on stellar surfaces only moderate. Temperature of the conventional laboratory plasmas ranges from a few thousand to milllons of degrees. The temperatures of our cold plasmas are as low as 133°C.

Finally since the cold plasma is a gas under equilibrium, the plasma lifetime is limited only by the non-plasma problem of self-reaction. Lifetimes of an hour have been attained. We feel that it may be possible to extend these lifetimes by at least an order of magnitude.

6. ACKNOWLEDGMENTS

It is a pleasure to acknowledge the assistance given by Kurt R. Fasold (glassblowing, purification and sample preparation), Wayne A. Schindler and Henry A. May (machining, design and fabrication of bomb assembly), and E. Mark Gold (physics, design of the conductivity measuring system).

7. REFERENCES

1880

80 HAN — Hannay and Hogarth, Proc. Roy. Soc. (London) 29, 324 (1879), 30, 178 (1880).
"On the Solubility of Solids in Gases."

1897

97 CAD — H. P. Cady, J. Phys. Chem. 1, 707-13 (1897).
"The Electrolysis and Electrolytic Conductivity of Certain Substances Dissolved in Liquid Ammonia."

1900

00 FRA — E. C. Franklin and C. A. Kraus, Am. Chem. J. 23, 277-313 (1900).
"The Electrical Conductivity of Liquid Ammonia Solutions."

00 FRA-a — E. C. Franklin and C. A. Kraus, Am. Chem. J. 24, 83-93 (1900).
"The Conductivity Temperature Coefficient of Some Liquid Ammonia Solutions."

1920

20 GRI — A. A. Griffith, Trans. Roy. Soc. London, A221, 163 - 198 (1920).
"The Phenomena of Rupture and Flow in Solids."

1921

21 KRA — C. A. Kraus, J. Am. Chem. Soc. 43, 749-70 (1921).
"Solutions of Metals in Non-Metallic Solvents. VI. The Conductance of the Alkali Metals in Liquid Ammonia."

1921

21 KRA-a C. A. Kraus and W. W. Lucasse, J. Am. Chem. Soc. 43, 2529-39 (1921).
"Conductance of Concentrated Solutions of Sodium and Potassium in Liquid Ammonia."

1922

22 KRA C. A. Kraus and W. W. Lucasse, J. Am. Chem. Soc. 44, 1941-49 (1922).
"The Resistance-Temperature Coefficient of Concentrated Solutions of Sodium Liquid Ammonia."

22 KRA-a C. A. Kraus, Chemical Catalog Co. 1922.
"The Properties of Electrically Conducting Systems."

22 LUC W. W. Lucasse, Pg. 83 in (22 KRA-a).

1923

23 KRA C. A. Kraus and W. W. Lucasse, J. Am. Chem. Soc. 45, 2551-55 (1923).
"The Resistance-Temperature Coefficient of Concentrated Solutions of Potassium in Liquid Ammonia and the Specific Conductance of Solutions of Potassium in Liquid Ammonia at Intermediate Concentrations."

1928

28 KIS G. B. Kistiakowsky, J. Am. Chem. Soc. 50, 2315 (1928).

1929

29 JOH W. C. Johnson and W. C. Fernelius, 6, 23-35 (1929). "Liquid Ammonia as a Solvent and the Ammonia System of Compounds. IV. Experimental Procedures Involved in the Manipulation of Liquid Ammonia Solutions."

1932

32 BIR F. Birch, Phys. Rev. 41, 641-8 (1932). "The Electrical Resistance and the Critical Point of Mercury."

1949

49 NÄB M. Näbauer, Z. angew. Physik 1,423-8 (1949). "Widerstandmessungen an Natrium-Ammoniaklösungen bei teifen Temperaturen."

1951

51 GIL P. T. Gilbert, Jr., Science 114, 637-40 (1951). "Silicone Water-Repellents for General Use in the Laboratory."

1957

57 EVE E. C. Evers, A. E. Young III, And A. J. Panson, J. Am. Chem. Soc. 79,5118-20 (1957). "Solutions of Metals in Amine Solvents. I. The Conductance of Concentrated Solutions of Lithium in Methylamine."

1960

60 BER D. S. Berns, E. C. Evers and P. W. Frank, Jr., J. Am. Chem. Soc. 82, 310-14 (1960).

"Solutions of Metals in Amine Solvents. III. The Conductance of Dilute Solutions of Lithium in Methylamine at -78.3°."

60 KOH W. H. Kohl, Reinhold, 1960.
"Materials and Techniques for Electron Tubes."

60 PAN A. J. Panson and E. C. Evers, J. Am. Chem. Soc. 82, 4468-71 (1960).
"Solutions of Metals in Amine Solvents. IV. The Effect of Temperature on the Conductance of Lithium in Methylamine."

1961

61 BEZ M. A. Bezborodov and A. M. Kripskiy (1961).
(Translation, March 1962, ASTIA AD No. 273 047).
"Ways of Obtaining Super-strong Unbreakable Glass."

1962

62 DON E. E. Donaldson, Vacuum 12, 11 (1962).

62 HOL J. H. Holley, G. R. Neff, F. B. Weiler and P. N. Winslow, Amer. Rocket Soc. Preprint No. 2386-62.
"Corrosivity and Contamination of Cesium in Ion Propulsion."

TABLE I

LOW TEMPERATURE DATA*

Sample No.	Mole Fraction of Na at -33.5°C	Specific Conductivity at 20°C, $ohm^{-1}\ cm^{-1}$	Cond. Cell Calib. Methods **	Resistance Measuring Method ***	Frequency kc
3-26-18	1.17×10^{-1}	2.43×10^{3}	G	V_o	5
3-26-10	5.32×10^{-2}	3.86×10^{2}	G	E	7
3-26-15	5.20×10^{-2}	3.70×10^{2}	G	V_o	7
4-26-8	5.14×10^{-2}	3.60×10^{2}	P	E	4
10-3-1A	5.04×10^{-2}	3.40×10^{2}	G	V_o	10
3-26-12	4.60×10^{-2}	2.65×10^{2}	G	E	7
33	4.04×10^{-2}	1.76×10^{2}	I	E	40
3-26-9	3.89×10^{-2}	1.48×10^{2}	G	V_o	10
4-26-2	3.59×10^{-2}	7.37×10	P	E	20
10-8-4	2.97×10^{-2}	6.45×10	G	E	1250
11-9-1A	2.92×10^{-2}	5.40×10	G	G	125
28	2.85×10^{-2}	3.40×10	I	E	50
26	2.81×10^{-2}	3.22×10	I	E	50
4-26-1	2.47×10^{-2}	2.10×10	P	E	80
10-30-3A	2.28×10^{-2}	1.35×10	G	G	200
3-26-16	1.89×10^{-2}	7.40	G	V_o	200
4-26-7	1.63×10^{-2}	4.30	P	E	400
4-26-5A	1.65×10^{-2}	3.85	P	V_o	400
4-26-3	1.34×10^{-2}	1.95	P	V_o	800
29	1.30×10^{-2}	1.86	I	E	800
9-5-4A	1.19×10^{-2}	1.43	G	E	1250
3-26-17	1.09×10^{-2}	9.35×10^{-1}	G	V_o	900
10-3-3	6.62×10^{-3}	5.20×10^{-1}	G	E	1250
X-15	5.48×10^{-3}	3.75×10^{-1}	G	G	125
10-8-4A	2.94×10^{-3}	1.56×10^{-1}	G	E	1250
10-8-3	1.74×10^{-3}	1.17×10^{-1}	G	E	1250

* All cells are made of pyrex except 11-9-1A, 26, 28, 29, and 33, which are fabricated from uranium glass.

** Conductivity cell calibration methods: G - Geometrical, P - DC Plunger, I - Inductive

*** Resistance Measuring Methods:

G - Graphical (R vs. Vo at fixed frequency and input voltage)

Vo - Constant transfer function $\frac{RV^{o}}{\sqrt{Vi}} = B$

E - External Calibrator

TABLE II

DATA FROM 20 TO 130°C*

Sample No.	Mole Fraction of Na at -33.5°C	Resistance** Measuring Method	Specific Conductance at 80°C, ohm^{-1} cm	Conductivity Maxima Temperature, °C	Conductivity Maxima σ, ohm^{-1} cm^{-1}
3-26-15	5.20×10^{-2}	Vo	4.70×10^{2}		
3-26-12	4.60×10^{-2}	Vo	3.32×10^{2}		
9-5-3A	3.37×10^{-2}	G	1.87	110	2.10×10^{2}
8-22-2A	3.22×10^{-2}	G	1.60	111	1.73×10^{2}
11-9-1A	3.00×10^{-2}	G	1.44×10^{2}	86	1.45×10^{2}
10-30-4	2.78×10^{-2}	G	9.9×10	81	9.90×10
10-3-4	2.57×10^{-2}	G	6.5	81	6.50×10
11-9-3	2.53×10^{-2}	G	6.25	94	6.60×10
10-30-3A	2.273×10^{-2}	G	3.68	95	3.80×10
10-3-2	2.10×10^{-2}	G	3.68	95	3.80×10
10-30-2A	2.01×10^{-2}	E	2.71	88	2.78×10
11-9-4	1.97×10^{-2}	G	2.23	95	2.32×10
10-3-3A	1.82×10^{-2}	G	1.76	97	1.90×10
10-3-2A	1.73×10^{-2}	G	1.44	93	1.51×10
10-3-5A	1.70×10^{-2}	G	1.25×10	98	1.33×10
3-26-14	1.35×10^{-2}	Vo	6.40	98	7.00
9-5-4A	1.192×10^{-2}	Vo	3.93	93	4.10
W-1	1.17×10^{-2}	G	3.45	92	3.53
10-30-3	7.1×10^{-3}	G	2.16	92	2.22
10-3-3	6.95×10^{-3}	Vo	1.52	86	1.53
10-3-4A	3.50×10^{-3}	G	3.05×10^{-1}	86	3.07×10^{-1}
9-5-1A	2.40×10^{-3}	E	1.30×10^{-1}	84	1.31×10^{-1}

* All conductivity cells in this table were calibrated by the geometrical technique.

** Resistance Measuring Method:

G - Graphical (R vs. Vo at fixed frequency and V^i)

Vo - Constant transfer function $\frac{RV^o}{\sqrt{V^i}}$

E - External Calibrator

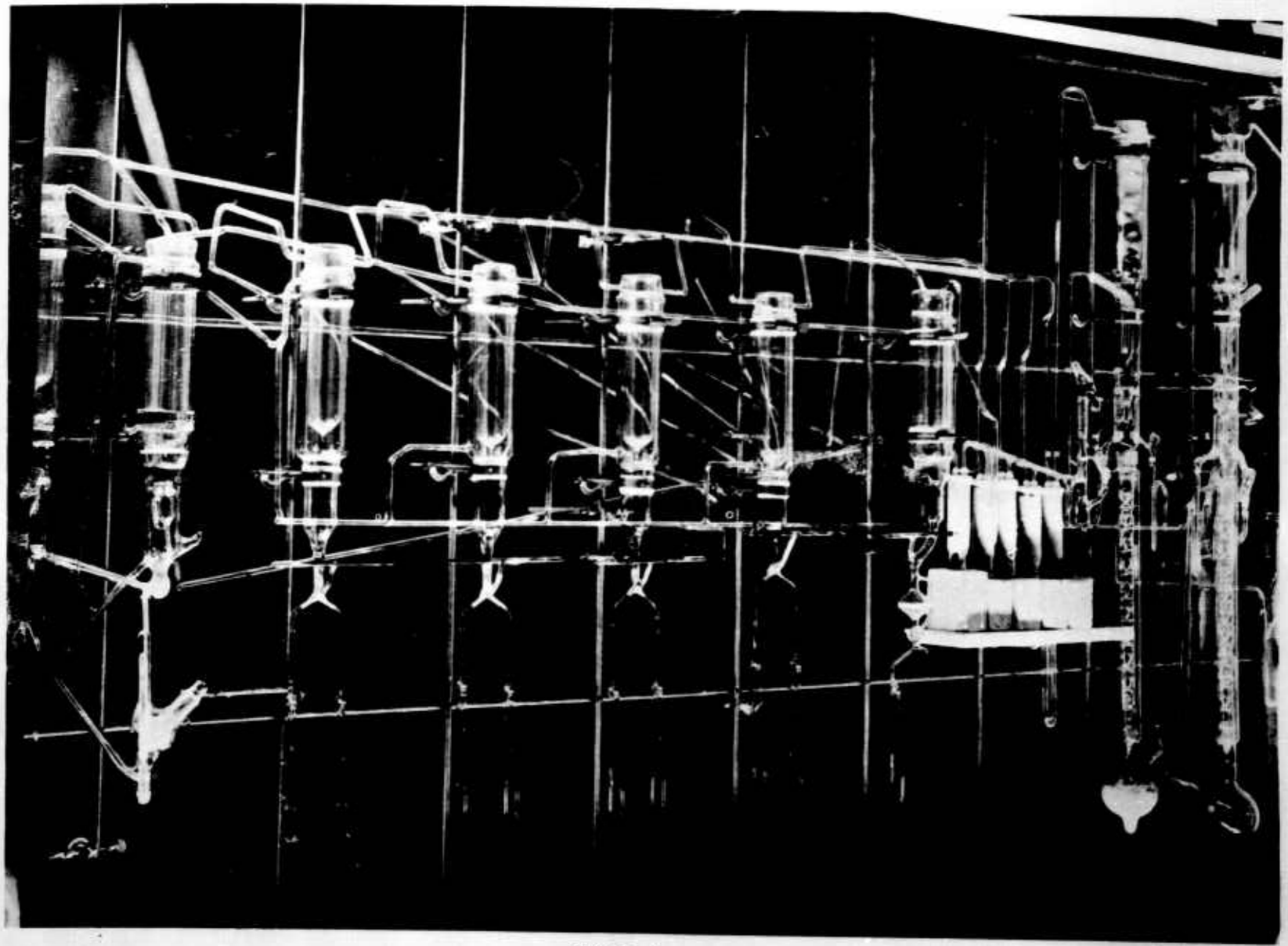

FIGURE 1

Ammonia Purification and Sample Preparation System

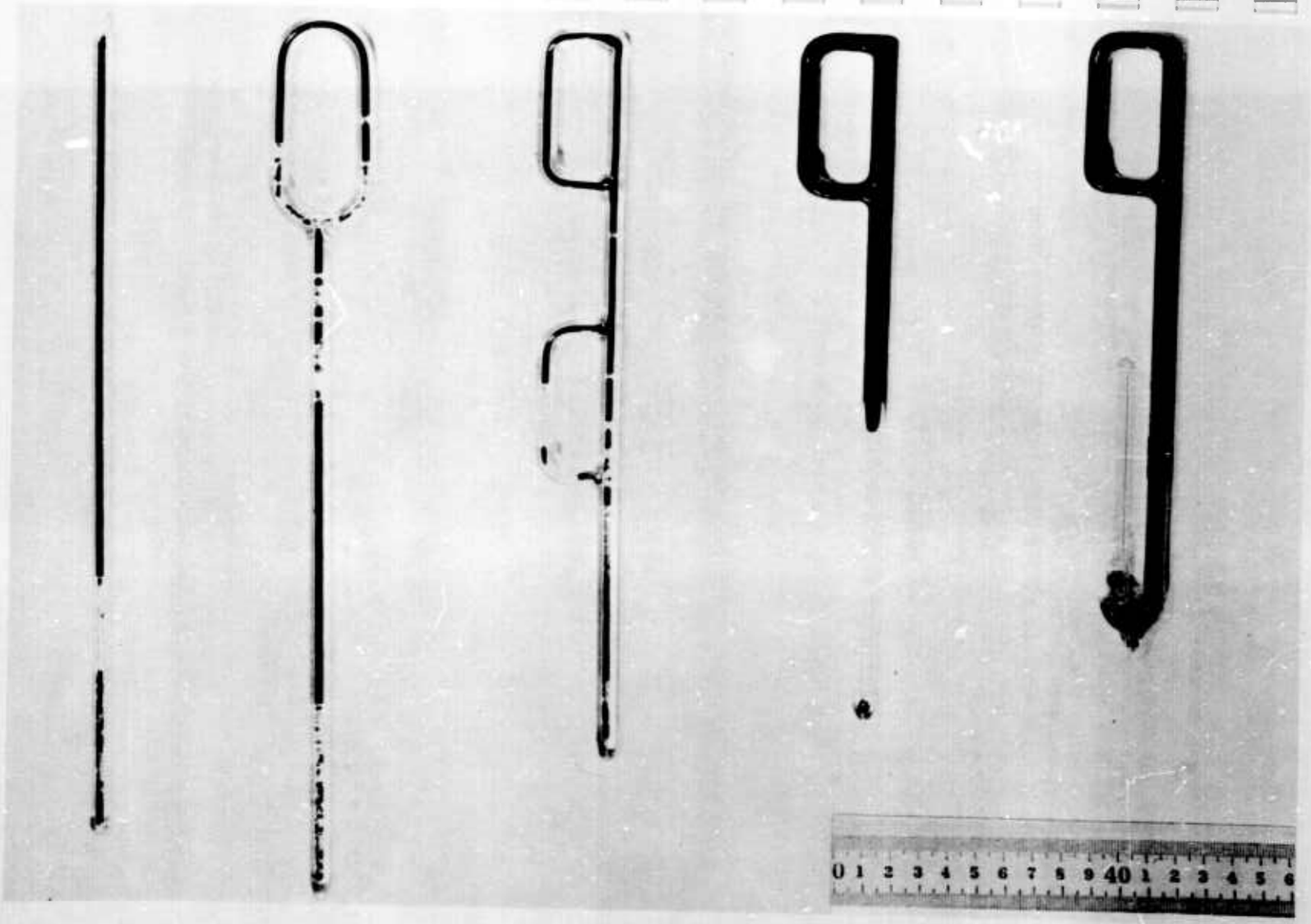

FIGURE 2 - LIFETIME AND CONDUCTIVITY CELLS

The first cell on the left is a heavy wall capillary used for visually observing lifetimes at elevated temperature. The second cell is a capillary conductivity cell allowing visual inspection. The third cell was designed for measuring conductivities at several positions along the cell to study uniformity of conductivity when using the bomb. The fourth cell is a large-bore conductivity cell used in the bomb. In the last cell, a breakseal is built on for purposes of gas analysis.

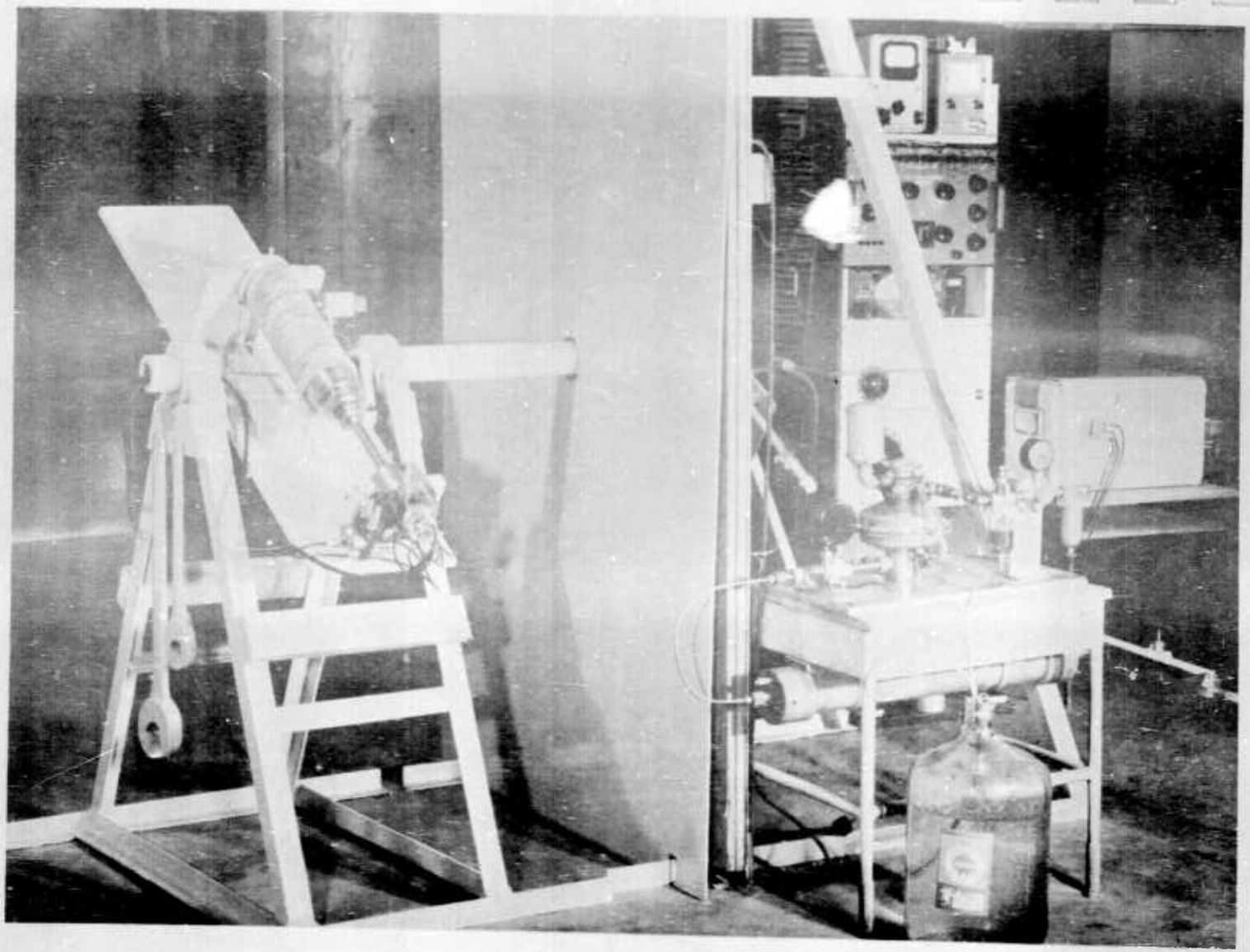

FIGURE 3 - THE HIGH TEMPERATURE CONDUCTIVITY MEASURING SYSTEM

The conductivity cell is inside the bomb located on the rotary table at the left of the safety shield. Rotation of the bomb table, heating, and measurements are all controlled from the right.

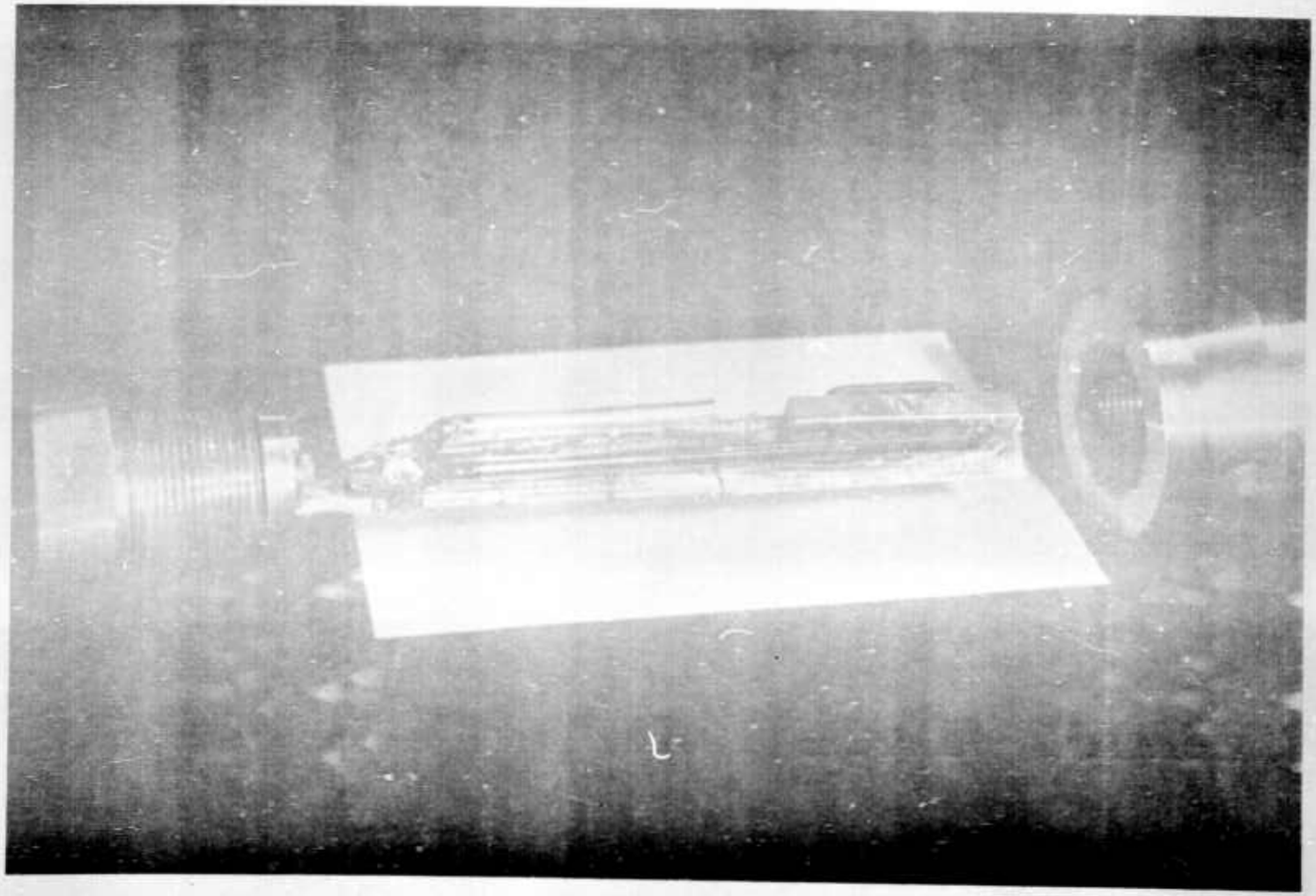

FIGURE 4 - CONDUCTIVITY ASSEMBLY INSIDE BOMB

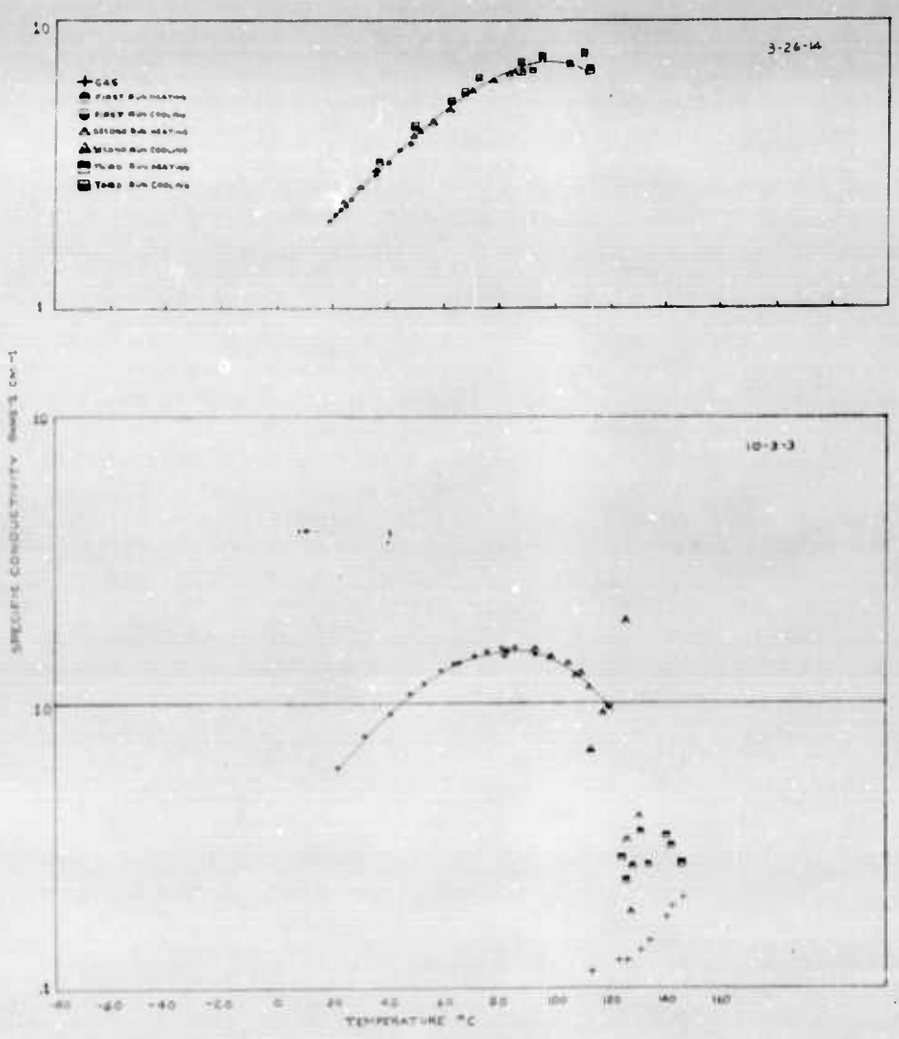

FIGURE 5 - REPRODUCIBILITY

Two test runs are shown, each of which was heated three separate times. There is no evidence of decomposition within experimental error for either run.

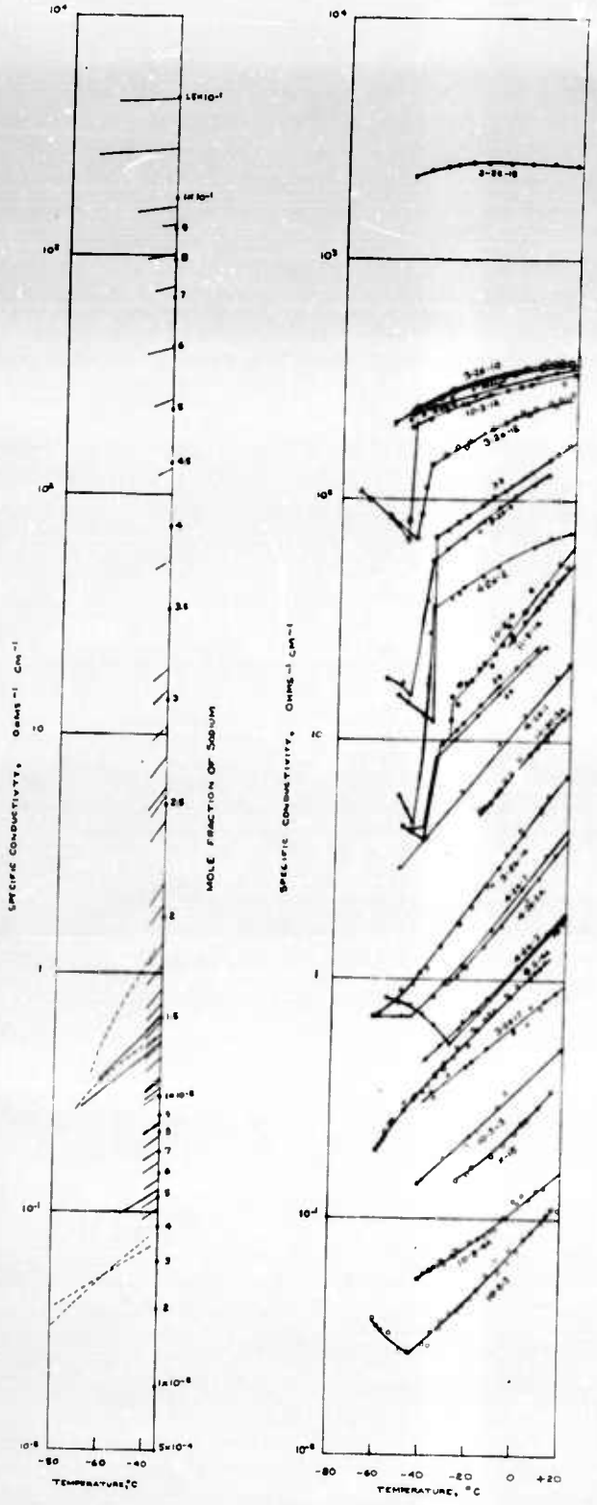

FIG 6

FIGURE 6 - ELECTRICAL CONDUCTIVITY TEMPERATURE DATA BELOW ROOM TEMPERATURE

The solid lines on the figure on the left are from the data of Kraus and Lucasse (22 KRA), the dashed lines being from Nabauer (49 NAB). The composition scale, mole fraction of sodium, is from the data of Kraus (21 KRA) and Kraus and Lucasse (21 KRA-a). Our conductivity temperature data below room temperature are displayed in the figure on the right.

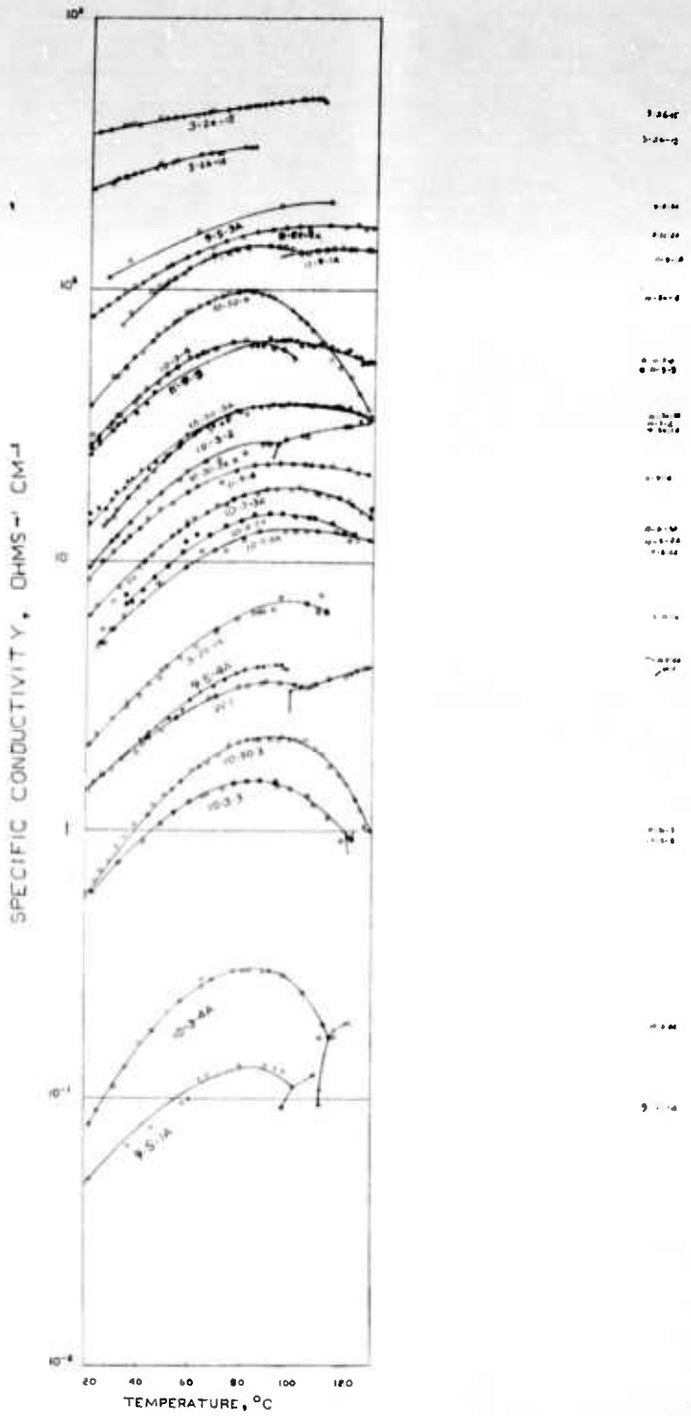

FIGURE 7 - ELECTRICAL CONDUCTIVITIES - TEMPERATURE DATA TO 130°C

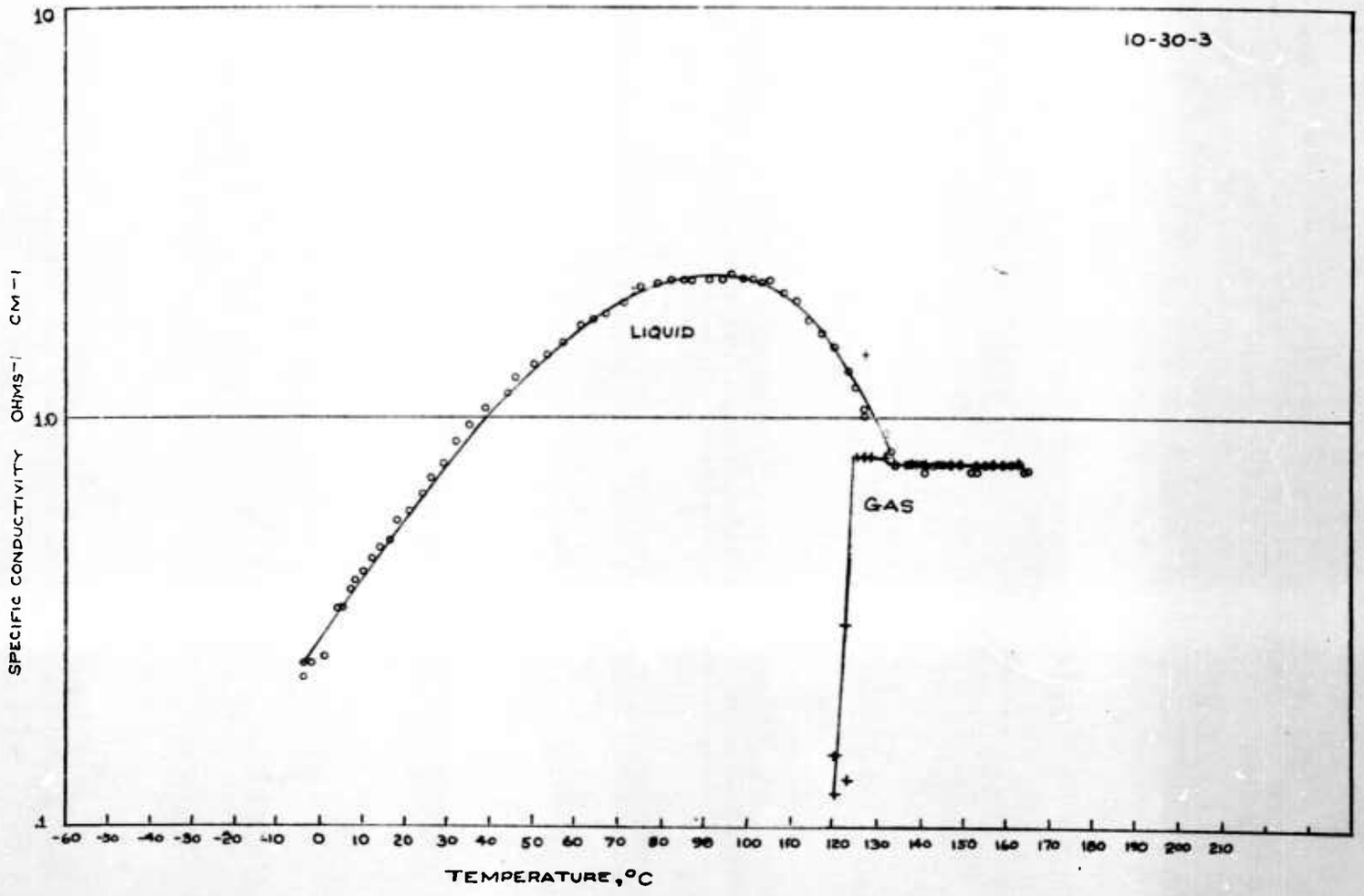

FIGURE 8 - CONDUCTIVITY TEMPERATURE DATA EXTENDING INTO THE GAS PHASE REGION

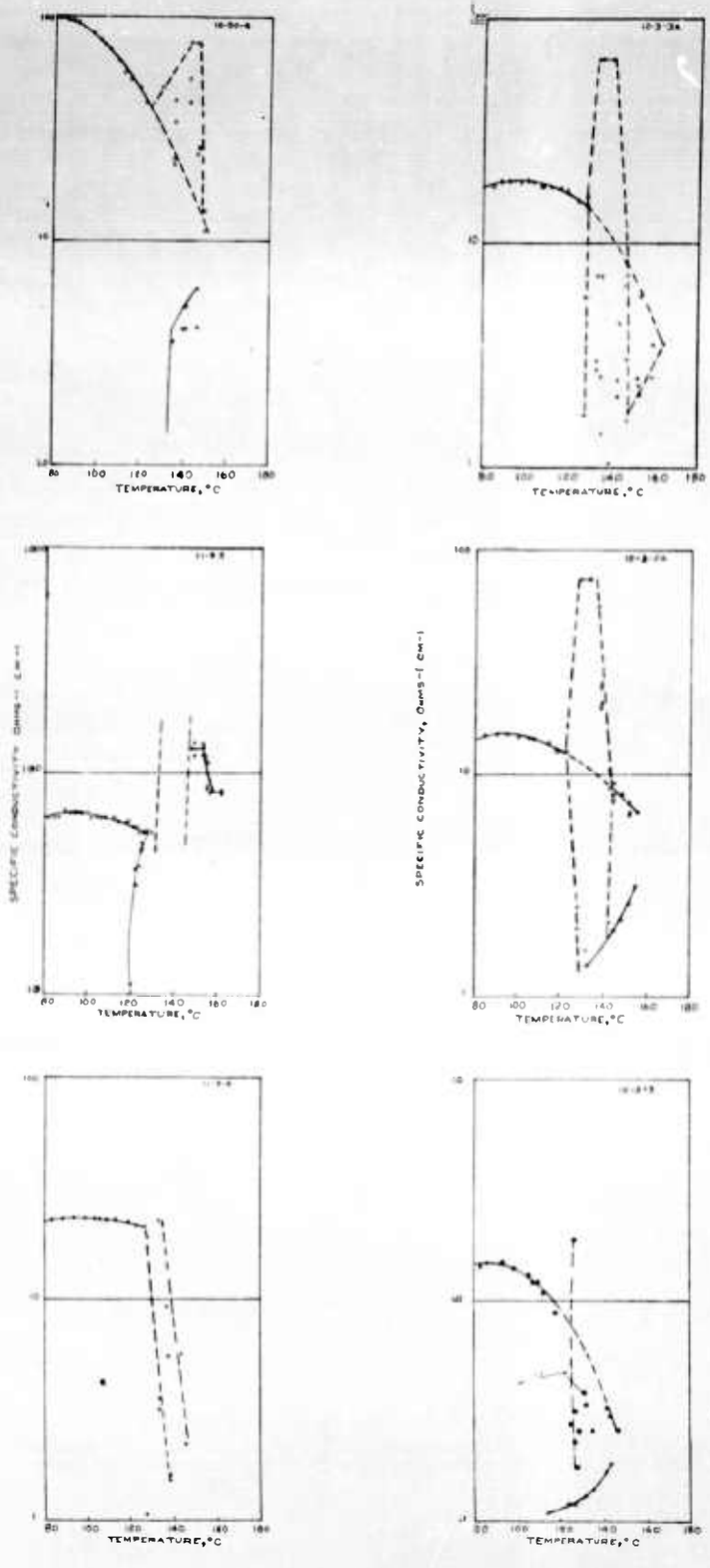

FIGURE 9 - TURBULENCE IN THE NEIGHBORHOOD OF THE CRITICAL REGION

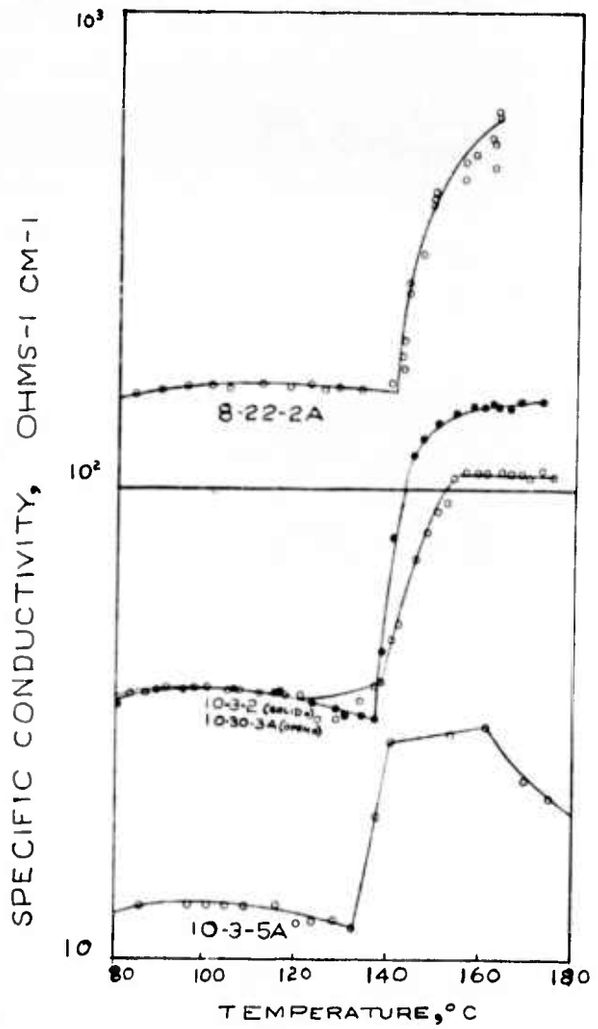

FIGURE 10 - CONDUCTIVITIES OF CONCENTRATED SOLUTIONS AT ELEVATED TEMPERATURES

UNCLASSIFIED